European Congress on Computational Methods
in Applied Sciences and Engineering (ECCOMAS 2012)
J. Eberhardsteiner et.al. (eds.)
Vienna, Austria, September 10-14, 2012

QUANTITATIVE ASSESSMENT OF RANDOM FIELD MODELS IN FE BUCKLING ANALYSES OF COMPOSITE CYLINDERS

V. De Groof[1], M. Oberguggenberger[1], H. Haller[2], R. Degenhardt[3] and A. Kling[3]

[1]Institut für Grundlagen der Bauingenieurwissenschaften, Universität Innsbruck
Technikerstraße 13, 6020 Innsbruck, Austria
e-mail: {vincent.de-groof,michael.oberguggenberger}@uibk.ac.at

[2]INTALES GmbH
Innsbrucker Straße 13, 6161 Natters, Austria
e-mail: haller@intales.com

[3]Institut für Faserverbundleichtbau und Adaptronik, DLR
Lilienthalplatz 7, 38108 Braunschweig, Germany
e-mail: {richard.degenhardt,alexander.kling}@dlr.de

Keywords: Random fields, Monte Carlo simulation, buckling analysis, composite shells.

Abstract. *Large scatter characterizes the collapse load of thin-walled structures due to their imperfection sensitivity. Random fields can be used to include imperfections in a finite element model, which can highly increase the credibility of the finite element (FE) model. Principal component analysis (PCA) and analytical covariance functions are matched to available correlation information of geometrical imperfection measurements. The random fields are realized by Karhunen-Loève expansion combined with Monte Carlo methods.*

The results of the different covariance models are compared with the deterministic collapse loads of the measured imperfections in the FE-model. This approach isolates the effect of the different covariance models from other inaccuracies such as boundary conditions, loading imperfections, etc.

The results show that random fields can be used to improve predictions and the understanding of the structural behavior of thin-walled structures, especially when these predictions are based on imperfection data, using PCA. Caution is recommended when using analytical covariance functions since they may fail to capture the complete behavior of the structure.

1 INTRODUCTION

The buckling load of thin-walled structures is known to be highly sensitive to imperfections. Imperfections in the loading, material properties, boundary conditions, geometry, etc. are all known to affect the buckling load of, in particular cylindrical, shells [1, 9]. Currently, knockdown factors are used to account for these uncertainties in industrial applications.

Knockdown factors are derived from experimental data from the 1960's and take the effects of all imperfections as a sum into account [11]. This makes it very hard to reduce the knockdown factor if one can reduce the uncertainty or imperfection of one or more design variables, as they are accounted for together. It is known that this often leads to overly conservative designs.

Nowadays, finite element software is widely used to determine the structural behavior of a given structure [13]. Detailed prediction of the buckling behavior of thin-walled structures requires a detailed and correct description of the imperfections. One needs a robust probabilistic framework and models that represent the imperfections to be modelled [6, 16].

In the past, random fields have been used to model imperfections. Geometry, thickness, material, loading, etc. have all been the subject of investigations using random fields [2, 12, 14]. Most of this research was based on the use of exponential covariance functions that were fitted to measurement data in a limited number of cases.

It is the writers' opinion that the verification of such models is lacking in the literature. Currently, these models are compared to the experimental failure loads. However, by comparing with the experimental failure load, the quality of the complete finite element model is evaluated, not the quality of the random field model. In such a comparison, it is tempting to attribute the differences to other uncertainties that were not taken into account, e.g. loading or boundary conditions. In contrast to this, the comparisons reported in this paper were done with respect to the deterministic imperfections applied to the finite element model. The differences between the models are now reduced to the way the imperfections were created; in this way, the effect of different descriptions of the random variations are isolated. This admits the assessment of the accuracy of the stochastic models in capturing the random influences as well as their predictive power.

The plan of the paper is as follows. In sections 2 and 3, the probabilistic framework is described that has been used to evaluate the data and generate the input samples for the finite element analysis. In section 4, details about the nonlinear finite element analysis are described. Section 5 is the central part of the paper in which our findings and conclusions about the different approaches are reported.

2 PROBABILISTIC FRAMEWORK

In the paper, the analysis of the data and the simulation of random fields is based on the Karhunen-Loève expansion as well as on principal component analysis. A direct Monte Carlo simulation approach was used to generate the samples for the finite element computations. Due to the rather high computational cost, the analysis has to be performed with small sample size N. In such a situation it is mandatory to use correlation control in order to improve the empirical independence of the generated random variables. These ingredients will now be described in more detail.

2.1 The Karhunen-Loève expansion

The Karhunen-Loève expansion decomposes a second order stochastic process U into a set of orthonormal deterministic functions, based on the eigenvalues and eigenvectors of its:

$$U(\mathbf{x},\omega) = g(\mathbf{x}) + \sum_{n=0}^{\infty} \sqrt{\lambda_n}\xi_n(\omega)\phi_n(\mathbf{x}) \tag{1}$$

where $\xi_n(\omega)$ is a sequence of random variables determined by the process, $g(\mathbf{x})$ is the mean function and λ_n and $\phi_n(x)$ are the eigenvalues and eigenvectors, respectively, of the eigenvalue problem

$$\int_W C(\mathbf{x}_1,\mathbf{x}_2)\phi_n(\mathbf{x})d\mathbf{x}_1 = \lambda_n\phi_n(\mathbf{x}_2) \tag{2}$$

where W is the domain, $C(\mathbf{x}_1,\mathbf{x}_2)$ is the covariance function. The covariance function $C(\mathbf{x}_1,\mathbf{x}_2)$ is symmetric and positive definite. The Karhunen-Loève expansion converges in the mean square sense. After truncating the expansion to a finite number of terms M, taking account of the M largest eigenvalues and eigenvectors will give a sufficiently small mean square error.

This property of the Karhunen-Loève expansion can reduce the computational effort related to solving the eigenvalue problem considerably since only the M largest eigenvalues and their corresponding eigenvectors are necessary. Especially highly correlated (low rate of change over the field) stochastic processes have rapidly decaying eigenvalues.

It is assumed here that the process U is Gaussian. Then the random variables $\xi_n(\omega)$ are independent and identically distributed according to a standard normal distribution. If the Gaussian assumption is dropped, analyzing and simulating random fields becomes more difficult. The generation of non-Gaussian random fields can be based on transformation processes [5] or on updating the random variables in the Karhunen-Loève expansion iteratively [7].

2.2 Monte Carlo simulation

A direct Monte Carlo (MC) approach was used for the simulations. In this approach, an artificial sample of size N of the set of input variables is generated and the computational model is evaluated for each realization of the input. This results in a sample of size N of the output variable, which can be further analyzed statistically. This simple approach was chosen because it allows easy implementation of a random field generator and can be used in combination with the available, deterministic, finite element packages such as Abaqus or Marc to perform a non-linear buckling analysis [3]. The estimator error, when using MC simulation, behaves as

$$e_{MC} \sim \sqrt{\frac{1}{N}} \tag{3}$$

where N is the MC sample size. As one can see, the order of convergence does not depend on the number of input random variables. This property of the MC simulation is highly beneficial in combination with random fields or models involving a large number of random variables.

2.3 Correlation control

When the sample size is small and the number of variables involved is appreciable, the multivariate output of a random number generators typically is weakly to moderately correlated,

but not independent. To improve the performance of the analysis and reduce the number of necessary realizations, correlation control was applied.

Correlation control is an empirical method that was proposed by Iman and Conover [8]. A sample of size N of an n-dimensional random quantity is generated. This data is then assembled into an $N \times n$ matrix. The goal of correlation control is to generate a new sample X^* that has a predefined target correlation matrix K. In this case, the identity matrix is targeted since the goal is to minimize the correlation between the different input variables. In general, the empirical correlation matrix R_X will be different from K. At first, the van der Waerden matrix W is set up by:

$$W = \begin{pmatrix} w_1^{(1)} & \dots & w_1^{(n)} \\ \vdots & \ddots & \vdots \\ w_N^{(1)} & \dots & w_N^{(n)} \end{pmatrix} \tag{4}$$

where each column is a random permutation of the van der Waerden scores

$$\Phi^{-1}\Big(\frac{j}{N+1}\Big), \qquad j = 1, \dots, N. \tag{5}$$

The Cholesky factorizations of the target correlation matrix K and the empirical correlation matrix R_X are defined by:

$$K = PP^{\mathsf{T}}, \quad R_X = QQ^{\mathsf{T}}. \tag{6}$$

Using the Cholesky factorizations, a new matrix W^* can be calculated:

$$W^* = WQ^{-\mathsf{T}}P^{\mathsf{T}} \tag{7}$$

The matrix W^* has the target correlation structure K. Empirical investigations by Iman and Conover showed that the rank correlation matrix of the resulting W^* is close:

$$\rho_{W^*} \approx R_{W^*}. \tag{8}$$

The last step to create the new data matrix X^* is the rearrangement of the values in the columns of X corresponding to the rank order of the columns in W^*. It then follows that X^* approximately has the desired correlation structure K, at least for the ranks:

$$\rho_{X^*} = \rho_{W^*} \approx R_{W^*} = K. \tag{9}$$

Iteration of the algorithm explained above often yields better results closer to the target correlation matrix K.

3 STOCHASTIC PROBLEM FORMULATION

The Karhunen-Loève method delivers an expansion of the covariance functions into orthogonal deterministic functions. These orthogonal functions can be derived in various ways. Section 3.1 explains how analytical functions can be used to assemble a covariance matrix. Section 3.2 shows how, by using principal component analysis, the eigenfunctions can be obtained more directly.

3.1 Covariance functions

Since the covariance matrix models contain the information of the spatial imperfections, adequate modelling of the covariance matrix is key in producing reliable results. In the past, a variety of covariance models have been applied. To the writers' knowledge, a quantifiable comparison has, probably due to the lack of measurement data, not yet been reported in the literature.

In theory, every function that produces a symmetric, positive definite matrix can be used to assemble a covariance matrix. In the past, the exponential covariance function has often been proposed as a good representation of reality. It has also been stated that the exponential covariance function may give rise to difficulties due to its nondifferentiability at zero. Modified kernels have been proposed to alleviate this problem [15].

The exponential and Gaussian covariance functions for a homogeneous and isotropic random field are defined by equations (10) and (11), respectively:

$$C(h) = \sigma^2 \cdot \exp\left(-\frac{|h|}{L_c}\right) \tag{10}$$

$$C(h) = \sigma^2 \cdot \exp\left(-\frac{h^2}{L_c^2}\right) \tag{11}$$

where h is the distance between two points and L_c is the correlation length. The correlation length describes the variation of the random field. Since the geometrical imperfections that will be described by random fields are not necessarily isotropic, a slightly different representation is necessary for orthotropic random fields. If one assumes that the variation along different axes is independent, the correlation structure can be split along, e.g., the axial and circumferential direction:

$$C(r, \theta) = \sigma^2 \cdot c(r, \theta) = \sigma^2 \cdot c_r(r) \cdot c_\theta(\theta) \tag{12}$$

Here, $c_r(r)$ represents the correlation function along the axial direction and $c_\theta(\theta)$ the correlation function along the circumferential direction. An important issue in industrial applications with irregular geometry is the distance calculation over the surface. For surfaces with a sufficiently simple analytical expression, this is a trivial task. If such a representation is lacking, the assembly of the autocovariance matrix becomes computationally expensive.

One of the main advantages of using covariance functions is that one does not necessarily need imperfection data of the specific structure to assemble a covariance matrix and perform a random field analysis. Available imperfection data can be extrapolated to structures with different dimensions or even shapes. Whether these covariance functions can be an adequate representation of the imperfection will be investigated in section 5 of this paper.

3.2 Principal component analysis

Principal component analysis is a statistical technique that extracts the main modes from a set of observations that, together, account for the major portion of the variance present in the observations [10]. Just as with the Karhunen-Loève method, these modes can then be used in a truncated expansion for simulating random fields with the same statistical distribution as the observed imperfections.

The covariance matrix $C = C(x_i, x_j)$ is directly calculated from the measured data at the points (x_i, x_j) by

$$C(x_i, x_j) = \mathrm{E}\left(U(x_i), U(x_j)\right) - \mu_i \mu_j \tag{13}$$

where $\mu_i = \mathrm{E}(U(x_i))$ is the mean of the field at point x_i. Solving the following eigenvalue problem

$$CV = VD, \tag{14}$$

the eigenvectors in V will form the basis of the expanded process, with the eigenvalues in D representing the weight of each eigenvector. Again, only a limited M number of elements of the basis need to be included to represent the random process.

PCA has been widely applied in computational statistics, e.g. in data mining and image compression. The main disadvantage of this approach for use with random fields is the necessity for measurement data. It is hardly possible to extrapolate parameters from data available elsewhere and match it to the case at hand.

4 STRUCTURAL ANALYSIS

To evaluate the random field models, a finite element model to determine the failure load of a thin-walled cylinder was created. In this comparative study, the measured geometrical imperfections were used as input of the FE model on the one hand; on the other hand, simulated imperfections based on the different random field models were entered in the FE calculations.

4.1 Nonlinear finite element analysis

When investigating the buckling behavior of thin-walled structures, large displacements arise. Assuming small displacements and executing a linear buckling analysis will give inaccurate results. A nonlinear analysis is necessary to make a prediction of the failure load.

Because of the large instability of the problem and the necessity to decrease the user input during the analysis as much as possible a loading-driven arc-length approach was used. Failure of the structure was defined by the occurrence of a loaddrop of 20% compared to the highest load reached during the previous steps. The highest load reached during the analysis is defined as the failure load. The analysis was ended when failure occurred; no post-buckling analysis was performed. This allows to assume that the strains remain small and therefore stay in the elastic regime.

4.2 Finite element type, boundary and loading conditions

Thin-walled structures are very sensitive to the applied boundary conditions and loading. Since the main goal of this research is the comparison of the random field models and not the accurate modelling of the real failure load, it was decided to use easy to model boundary conditions and loading. The evaluation of the model was done with respect to the results of the same finite element model where the measured imperfections were applied. This means that the only differences come from the models of the imperfections, but none are from the discrepancies between reality and the finite element model. Figure 1 shows a comparison of the different buckling loads for each cylinder.

Boundary conditions are applied at the top and bottom of the cylinder. For the bottom nodes, all the translational degrees of freedom are constrained. At the top the same boundary conditions are applied, but the axial direction is left free. In this direction, a compressive load is applied. The load is applied at the center of the cylinder and connected to all the top nodes using a multi-point constraint. A mesh convergence analysis showed that a mesh with around 11.000 elements was a good compromise between numerical accuracy and analysis time.

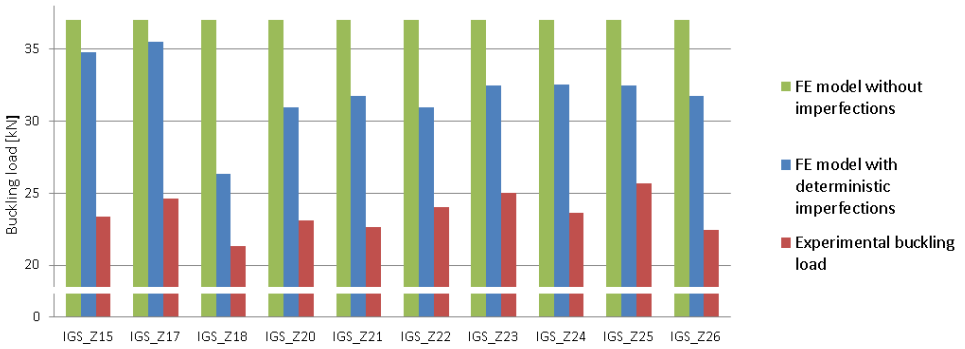

Figure 1: Comparison of the failure loads showing the discrepancies between finite element failure load predictions with and without geometrical imperfections and the experimental buckling load.

Property	Value
Radius	250mm
Height	500mm
Thickness	0.5mm
Layers	4
Lay-up	$24°/-24°/41°/-41°$

Table 1: Geometrical and lay-up properties of the cylinders.

Abaqus provides a large element library to solve a wide variety of structural problems. Since a thin-walled cylinder needs to be modelled, the S4 and S4R elements in the ABAQUS library are the most appropriate. The S4R element employs a reduced integration formulation and is therefore computationally more efficient. Because a comparative study showed that the gain in computational efficiency of the S4R element did outweigh the gain in accuracy of the S4 element, the S4R element was chosen.

4.3 Including the imperfections

The empirical data made available as a basis for this research [4] consisted of scans of the geometry of 10 cylinders made of composite material. The properties of the cylinders are shown in table 1. From these measurements, it was possible to derive the local imperfect radius of the cylinder at around 200.000 points per cylinder. Since the measurement mesh is too fine for the finite element computations and the correlation analysis, the data had to be broken down to the coarser FE mesh. Because the mesh is very fine, using the imperfect radius of the measured point closest to each grid point of the finite element description was judged to be enough. The imperfections were applied onto the finite element model using the **IMPERFECTION* option provided by ABAQUS. This option allows to include imperfections in the finite element model without getting errors about distorted elements.

5 RESULTS

5.1 Evaluating the random field model

The primary goal of this research was to assess the predictive quality of different approaches to modelling and creating random fields as representations of geometrical imperfections. The

comparisons following hereafter are made with respect to the failure loads of the finite element model with the measured geometrical imperfections directly applied to it. For reasons explained in the introduction, they are not compared directly to the experimental buckling loads.

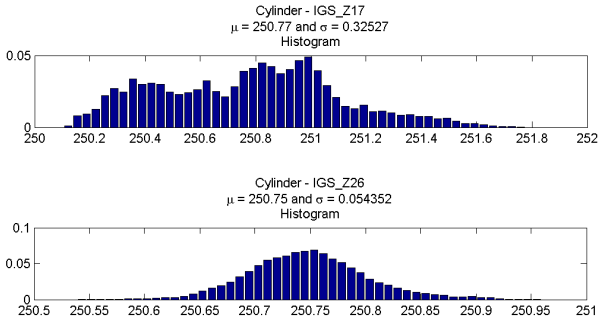

Figure 2: Two example histograms of two cylinders belonging to different sets.

5.2 The probability distribution

After investigation of the probability functions of the measurements it was found that the assumption of a Gaussian distribution is acceptable. Figure 2 shows the histograms of two measurements. While the Gaussian distribution is not immediately recognizable for the cylinder belonging to the top histogram in figure 2, the assumption holds in general for other realizations.

Set	Sample Size	Mean	Standard Deviation
Set 1	3	250.78	0.321
Set 2	6	250.73	0.068
Set All	9	250.75	0.152

Table 2: Average mean and standard deviation of the geometrical imperfections per set.

A more problematic observation is the large variation of the standard deviation of the local radii. Investigations showed that these can vary up to almost a factor ten. A closer investigation revealed two sets with distinctly different standard deviations. A visual investigation of the imperfections confirms the existence of these sets. Figure 3 shows the imperfect radius for two different cylinders which are both representative for a set. One can see that the two sets exhibit different imperfection structures, which is also confirmed by the calculation of the correlation functions in section 5.3. Based on this observation it was decided to divide the available sample in two different sets and to form the analysis separately (as well as jointly for comparison). The average mean and standard deviation of each set are reported in Table 2.

The visual inspection also revealed the existence of an outlier. Because it was impossible to make any assumptions about the reason for the deviating imperfection shape, it was decided to remove this realization from the available sample. This reduced the sample size from 10 to 9.

5.3 Theoretical covariance models

As one can see in figure 3, the imperfections are direction dependent. This observation was confirmed by calculating the correlation functions independently. Figure 4 shows the correlation

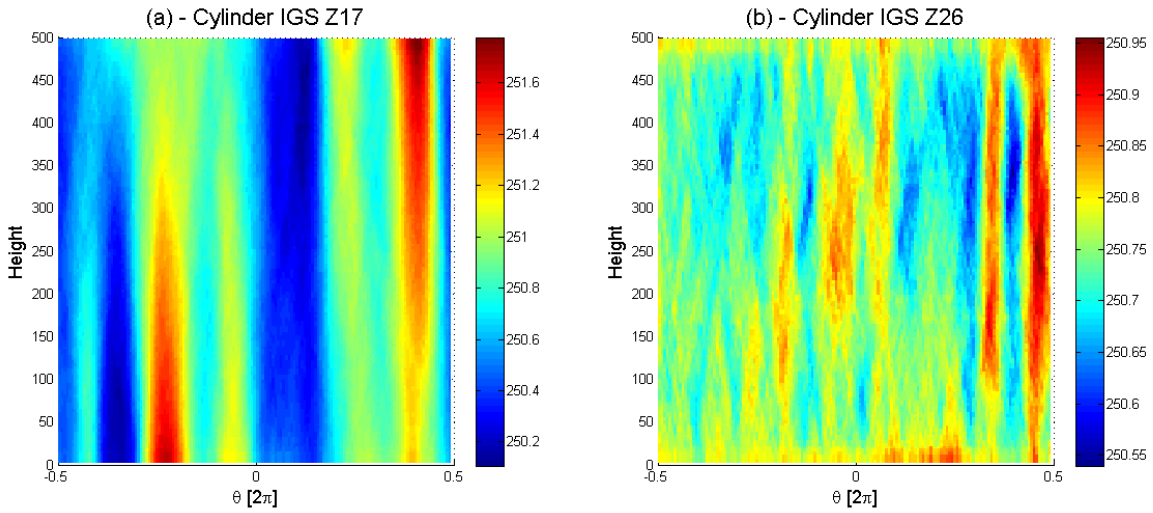

Figure 3: Geometrical imperfections of 2 cylinders. Cylinder IGS Z17 is part of set 1, cylinder IGS Z26 is part of set 2.

functions in axial and radial direction. The correlation is higher in the axial direction then in the radial direction. In axial direction, the cylinders are clearly different; set 2 has a lower correlation than set 1. It is less obvious from figure 3 that the correlation function in the radial direction is similar for both sets.

The theoretical correlation functions shown in table 3 have been fitted to the empirical correlation functions. The exponential correlation function gave the best fit in axial direction. The Gaussian correlation function did not fit well at $h = 0$ since the slope of the Gaussian correlation function is zero at this point. In radial direction, the mix of the cosine and the exponential correlation function gave the best fit.

Direction	Correlation function
Axial and radial	$c(r) = \exp\left(-\frac{\lvert r\rvert}{CL_{ax}}\right)$
Axial and radial	$c(r) = \exp\left(-\frac{r^2}{CL_{ax}^2}\right)$
Radial	$c(\theta) = \exp\left(-\frac{\lvert\theta\rvert}{CL_{rad}}\right) \cdot \cos\left(\frac{\lvert\theta\rvert}{P}\right)$
Radial	$c(\theta) = \exp\left(-\frac{\theta^2}{CL_{rad}^2}\right) \cdot \cos\left(\frac{\lvert\theta\rvert}{P}\right)$

Table 3: Fitted correlation functions.

Using these theoretical correlation functions, $N = 100$ random fields were generated and applied to the finite element model to evaluate the failure load. Figure 5 shows the resulting failure loads in a histogram compared to the deterministic failure loads of the imperfections. Additionally, the effect of the standard deviation was investigated. The appropriate standard deviations are 0.068 for set 1 and 0.321 for set 2.

When applying the correct standard deviations, it becomes clear that the theoretical correlation model overestimates the failure load. The effect of the standard deviation is twofold. Increasing the standard deviation not only reduces the average failure load, but also increases the spread of the failure load. The decrease of the failure load is limited compared to the in-

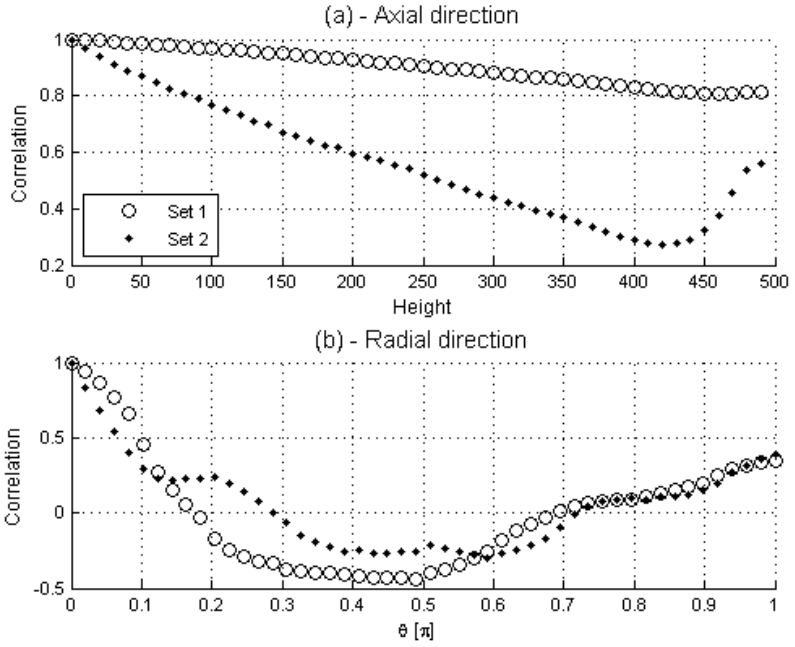

Figure 4: Empirical correlation functions of the geometrical imperfections in axial and radial directions.

crease of the standard deviation.

From this figure it also becomes clear that the effects of the different correlation functions are small, especially when one compares them with the effect of the standard deviation. If the correct standard deviation is applied, the functions consistently overestimate the failure load.

5.4 Principal component analysis

As an alternative to the theoretical covariance functions, PCA is proposed. When using PCA, the assumption enters that the given measurements are a valid (and complete) representation of the main characteristics of the imperfections. As explained in section 3.2, PCA obtains the eigenvectors and eigenvalues directly from the covariance matrix of the available measurements. These eigenvectors and eigenvalues can then be used in an orthogonal expansion to assemble the random fields.

The results from the Monte Carlo simulation are summarized in figure 6. The effect of the standard deviation has also been investigated. As one can see from this figure, the effect of the different standard deviations remains the same as for the theoretical correlation functions; the average failure load decreases and its standard deviation increases.

But the predictions are better when using PCA to obtain the eigenvectors and eigenvalues – especially in the case of set 2, where the standard deviation of the failure loads of the available realizations is small compared to set 1.

The predictions of set 1 are worse compared to set 2. An important cause for this behavior is probably the large standard deviation of the failure loads with the deterministic imperfections and the very small sample size of only 3 realizations. The main characteristics of the geometrical imperfections in this case probably do not coincide with the main driver for failure.

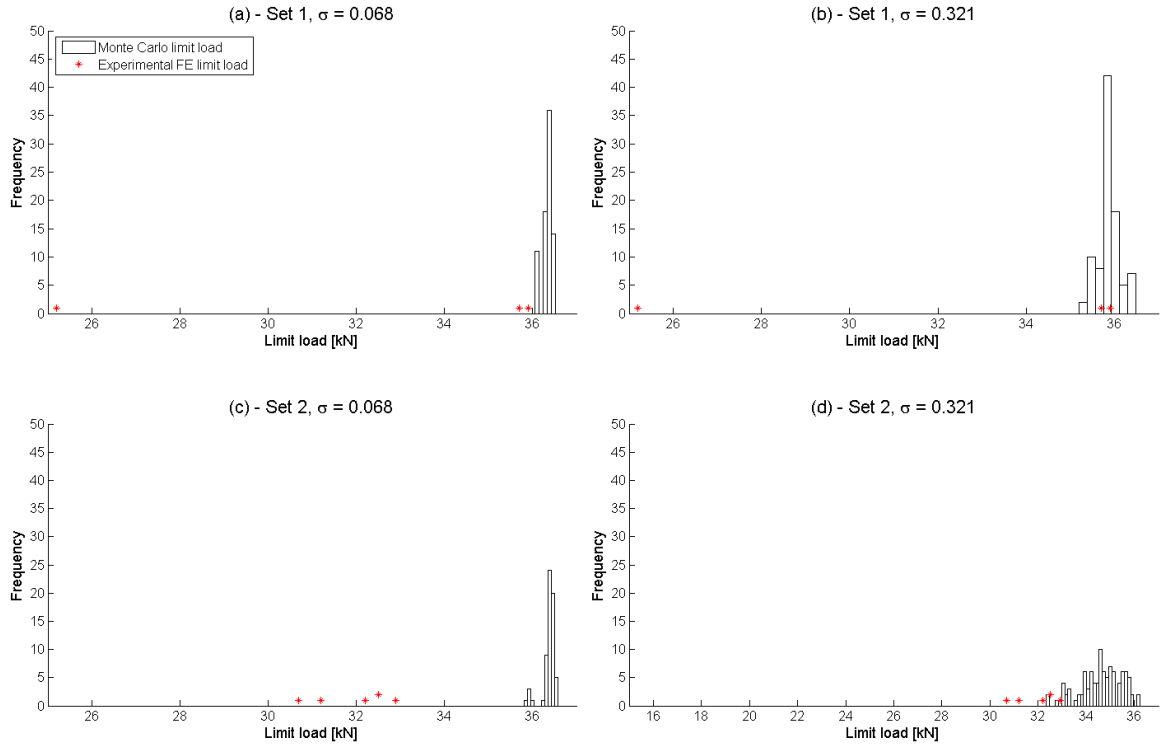

Figure 5: Histograms of the failure load of a theoretical covariance function with independency assumed along axial $\left(c(r) = \exp\left(-\frac{|r|}{CL_{ax}}\right)\right)$ and radial $\left(c(\theta) = \exp\left(-\frac{|\theta|}{CL_{rad}}\right) \cdot \cos\left(\frac{|\theta|}{P}\right)\right)$ direction, under the influence of different standard deviations. Real standard deviation of set 1 is 0.321 and 0.068 for set 2.

5.5 Analysis without set partioning

To complete the investigations, a last comparison without partitioning into different sets was made. Figure 7 shows the failure loads when averaging the standard deviation of the imperfections. It can be observed that the PCA behaves better than the theoretical correlation function, that overestimates the failure loads. The PCA also has difficulties with reproducing the extreme failure loads.

In the previous comparison, the applied standard deviation was the average of all the measurements. Previously, it was shown that the standard deviation has a considerable effect on the failure load. Therefore, in a final study, the set of nine measurements was entered into the PCA. The simulations were performed with three different variances and 3N realizations. The results are shown in figure 8.

When using a variation of realistic standard deviations, almost all the failure loads produced by the deterministic imperfections are captured including the lowest one. The histogram shows asymmetry which can also be observed in the underlying measurements.

6 CONCLUSIONS

Different covariance models have been evaluated to check their validity to represent general geometrical imperfections. The models with random fields have been compared with the failure loads of the finite element model when the measured imperfections are applied. By comparing to the deterministic imperfect finite element failure loads, the effect of the geometrical imperfection is isolated from other influences, such as boundary or loading imperfections.

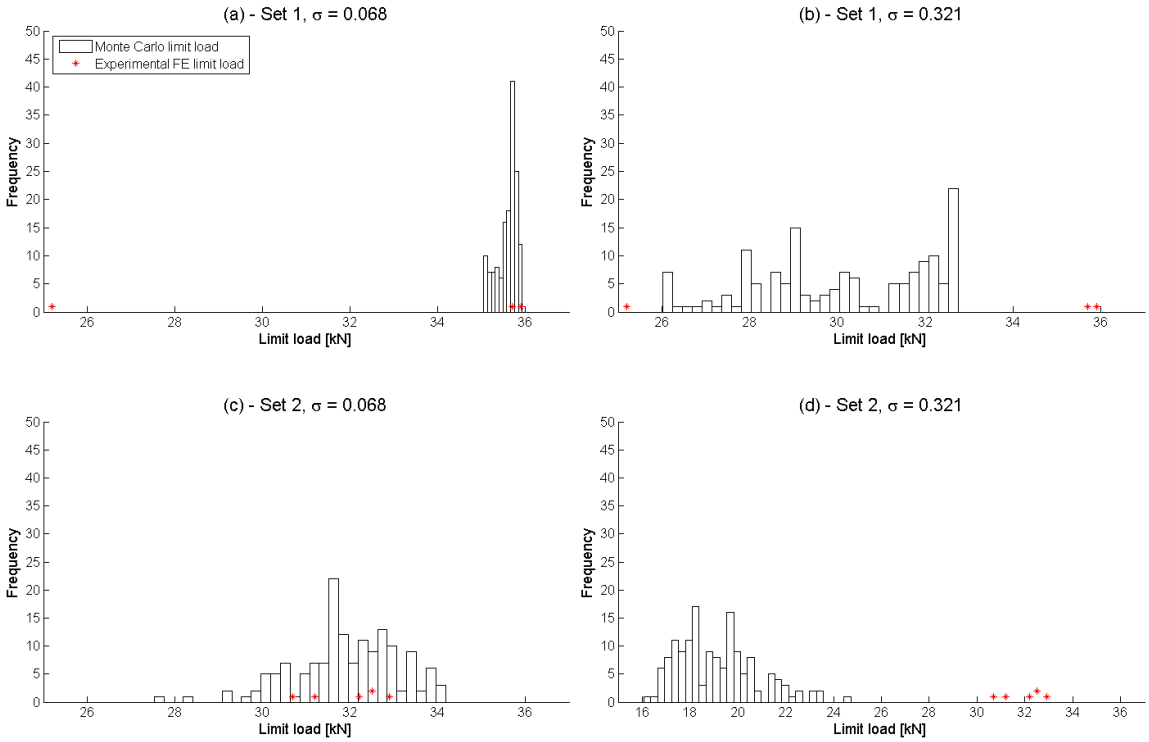

Figure 6: Histograms of the failure load of a PCA-analysis, under the influence of different standard deviations. Real standard deviations of set 1 and set 2 are 0.321 and 0.068, respectively.

It was shown that the theoretical covariance models overestimate the failure load and do not provide an accurate prediction of the failure load. The results of the PCA are better, but only work well when the sample size is large enough and the effect of varying standard deviation is taken into account. In this case, PCA is able to capture the lowest failure loads.

An overall conclusion is that it is important to validate stochastic models before applying them to engineering problems. A mere comparison of the computational results with the experimental buckling loads to evaluate correlation models may be misleading, especially for shells where different sources of imperfections can have a large influence on the resulting failure load. A better approach is a comparison with the measured imperfections applied to the finite element model.

REFERENCES

[1] J. Arbocz. The effect of imperfect boundary conditions on the collapse behavior of anisotropic shells. *International Journal of Solids and Structures*, 37(46-47):6891–6915, 2000.

[2] M. Broggi and G.I. Schuëller. Efficient modeling of imperfections for buckling analysis of composite cylindrical shells. *Engineering Structures*, 33(5):1796–1806, 2011.

[3] C. Bucher. *Computational analysis of randomness in structural mechanics*. CRC Press, Boca Raton, FL, 2009.

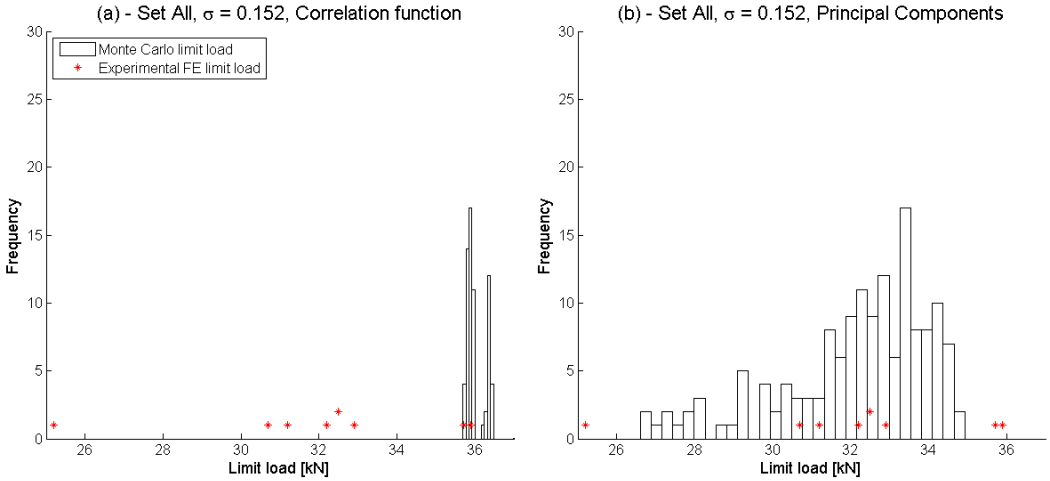

Figure 7: Histograms of the failure load of a PCA-analysis, using all 9 observations and averaged standard deviation.

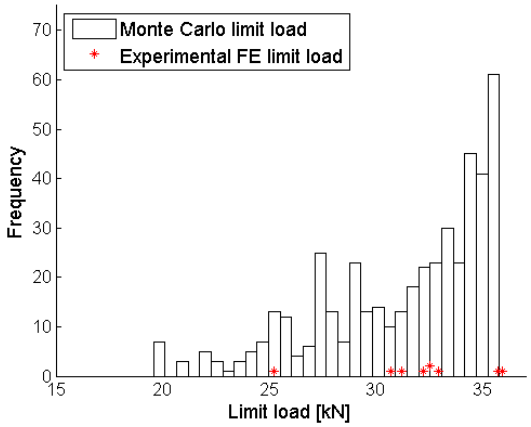

Figure 8: Histogram of the failure load of a PCA-analysis, without set division and using different standard deviations ($\sigma = 0.068$, $\sigma = 0.152$, $\sigma = 0.321$).

[4] R. Degenhardt, A. Kling, A. Bethge, J. Orf, L. Kärger, R. Zimmermann, K. Rohwer, and A. Calvi. Investigations on imperfection sensitivity and deduction of improved knock-down factors for unstiffened CFRP cylindrical shells. *Composite Structures*, 92(8):1939–1946, 2010.

[5] F.J. Ferrante, S.R. Arwade, and L.L. Graham-Brady. A translation model for non-stationary, non-Gaussian random processes. *Probabilistic Engineering Mechanics*, 20(3):215–228, 2005.

[6] R.G. Ghanem and P.D. Spanos. *Stochastic finite elements: a spectral approach*. Springer-Verlag, New York, 1991.

[7] S.P. Huang, K.K. Phoon, and S.T. Quek. Digital simulation of non-Gaussian stationary processes using Karhunen-Loève expansion. In *Proc. 8th ASCE Spec. Conf. Prob. Mech. & Struct. Reliability*, 2000.

[8] R.L. Iman and W.J. Conover. A distribution-free approach to inducing rank correlation among input variables. *Communications in Statistics-Simulation and Computation*, 11(3):311–334, 1982.

[9] J.F. Imbert. *The effect of imperfections on the buckling of cylindrical shells*. PhD thesis, California Institute of Technology, Pasadena, California, 1971.

[10] B. Lechner and M. Pircher. Analysis of imperfection measurements of structural members. *Thin-walled Structures*, 43(3):351–374, 2005.

[11] M.P. Nemeth and J.H. Starnes Jr. The NASA monographs on shell stability design recommendations. Technical report, Langley Research Center, Hampton, Virginia, 1998.

[12] V. Papadopoulos, G. Stefanou, and M. Papadrakakis. Buckling analysis of imperfect shells with stochastic non-Gaussian material and thickness properties. *International Journal of Solids and Structures*, 46(14-15):2800–2808, 2009.

[13] C.A. Schenk and G.I. Schuëller. *Uncertainty assessment of large finite element systems*, volume 24 of *Lecture Notes in Applied and Computational Mechanics*. Springer-Verlag, 2005.

[14] C.A. Schenk and G.I. Schuëller. Buckling analysis of cylindrical shells with cutouts including random boundary and geometric imperfections. *Computer Methods in Applied Mechanics and Engineering*, 196(35-36):3424–3434, 2007.

[15] P.D. Spanos, M. Beer, and J. Red-Horse. Karhunen–Loève expansion of stochastic processes with a modified exponential covariance kernel. *Journal of Engineering Mechanics*, 133:773, 2007.

[16] G. Stefanou. The stochastic finite element method: past, present and future. *Computer Methods in Applied Mechanics and Engineering*, 198(9-12):1031–1051, 2009.